Tetrahedron 66 (2010) 9123–9128

Contents lists available at ScienceDirect

Tetrahedron

journal homepage: www.elsevier.com/locate/tet

Atomic-scale determination of DNA conformational response to strained furanose: a static mode approach

Marie Brut [a,b,c,*], Alain Estève [a,b], Georges Landa [a,b], Ahmed Dkhissi [a,b], Guillaume Renvez [a,b], Mehdi Djafari Rouhani [a,b], David Gauchard [a,b]

[a] LAAS-CNRS, Université de Toulouse, 7 avenue du Colonel Roche, F-31077 Toulouse, France
[b] Université de Toulouse, UPS, INSA, INP, ISAE, LAAS, F-31077 Toulouse, France
[c] Department of Structural Biology, Stanford University School of Medicine, Stanford, CA, United States

ARTICLE INFO

Article history:
Received 29 June 2010
Received in revised form 14 September 2010
Accepted 15 September 2010
Available online 8 October 2010

Keywords:
Constrained nucleic acids
Furanose puckering
Induced-fit
Macromolecular flexibility
Atomic scale modeling

ABSTRACT

An original approach of macromolecular 'induced-fit' flexibility, namely the static modes, is applied to shed light on some fundamental mechanisms impacting DNA conformations. We first investigate a constrained nucleic acid of the D-CNA family, in which some backbone torsional angles are conformationally restricted by a dioxaphosphorinane ring structure. We take a special interest in α,β-D-CNA, in which α and β angles are restricted to the canonical conformation. We used the static mode method to evaluate the impact of the insertion of modified nucleotides on the stability of DNA/DNA and DNA/RNA duplexes. Although our approach authorizes the design of complex excitation modes on a specific molecule, we here establish with an atomic precision how a DNA south to north transition can be optimally operated through C5′ and O5′ single excitations.

1. Introduction

DNA is a flexible structure, animated by a complex set of parameters: intramolecular hydrogen bonds, electrostatic forces along the backbone, and with the ionic environment, interactions with specific proteins.[1,2]

On one hand, according to the concept of structural pre-organization,[3,4] rigidifying a molecule into a shape found in a complex facilitates the complex formation. Nucleic acids are crucial examples of preorganized structures as their intrinsic flexibility allows adapting themselves to interact with a wide range of molecules of different shape and nature. On the other hand, the overall DNA conformations, i.e., A, B or Z conformations can be defined through specific local structure peculiarities of its nucleosides,[5,6] opening exciting perspectives to monitor DNA structural behavior.

The particular case of modified nucleotides, preorganized to fit standard DNA or RNA duplexes, has attracted much interest in recent years[7–10] to improve the selectivity and specificity of nucleic acids strands. As they exhibit enhanced hybridization efficiency with a complementary strand, their insertion increases the thermal stability of duplexes. In locked nucleic acid (LNA),[11,12] the ribose ring is locked by a methylene bridge connecting the 2′-O and 4′-C atoms. In aqueous solution, double-stranded DNA is most of the time in a B-form, with sugars in a south (S) conformation, but can be found in the A-form when hydration conditions change or when submitted to an interaction within a complex. In this later case, sugars switch to the north (N) conformation. RNA duplexes are always found in the A-form.[6] Regarding these conformational differences between the nucleic acid forms, one way to preorganize their structure possibly relies on the sugar structure, i.e., on the conformational restriction applied to the sugar into S or N conformation. The purpose is to rigidify the sugar with a pucker similar to those observed in A- or B-form duplexes, so that the locked ribose conformation improves base stacking and backbone pre-organization. Many modified nucleosides have been synthesized these last years, opening the way to new and original pharmaceutical and technological perspectives.[13–16]

Whatever they are, these modifications are today impacting many research domains from standard molecular biology to advanced nanotechnologies. In this last area, examples of 'bio-inspired' materials include nucleic acid aptamers engineered through in vitro techniques to bind to a wide range of targets (biological or not),[17] selectivity being further improved through additional chemical modifications. It includes also Peptide Nucleic Acids (PNA), artificially synthesized to provide DNA like structures that have modified properties: DNA/PNA strand binding will be stronger

* Corresponding author. Tel.: +1 650 725 0754; fax: +1 650 723 8464; e-mail address: mbrut@stanford.edu (M. Brut).

0040-4020/$ – see front matter © 2010 Elsevier Ltd. All rights reserved.
doi:10.1016/j.tet.2010.09.083

than that of DNA/DNA strands.[18] These examples demonstrate that there is a major interest in understanding the basic mechanisms that are impacting DNA conformations enabling subsequent control of the DNA reactivity. Our purpose here is to shed light in these issues by using a static mode technique[19] that makes possible to map the DNA deformation response to specific and chosen external excitation with an atomic precision.

In the following, we consider a preorganized single-strand DNA in which rigidity is accomplished directly on the backbone with a conformationally restricted phosphate linkage:[20] some backbone torsion angles are locked in a dioxaphosphorinane ring structure (D-CNA),[21,22] as shown on Fig. 1b. Specifically, we focus on α,β-D-CNA, in which α and β torsion angles are restricted in a canonical conformation (α=*gauche*(−),β=*trans*). Such α,β-D-CNAs have been synthesized[23] and inserted into duplexes to evaluate their effect on thermal stability. It has been found that (α=*g*−; β=*t*) modifications inserted in a DNA duplex (B-form) increase significantly its stability,[24,25] much more than in a DNA/RNA heteroduplex (A-form). One hypothesis for this behavior is that the constrained nucleotide sugar (5′-sugar) is frozen and cannot switch from a south to a north conformation.

how we can determine the exact routes for DNA overall conformational changes through local furanose deformations.

2. Materials and method

2.1. The static mode method

Whereas changes of conformation are a key issue in biology, current algorithms are not adequate to explore the flexibility or large amplitude movements of macromolecules.[26] Introducing flexibility with an acceptable computational cost in already complex multi-level modeling strategies is a real challenge, and is essential to improve our understanding of both intrinsic properties of single molecule (folding) and interactions through the formation of macromolecular complexes (docking procedures).

Beyond the current challenge of considering the full flexibility in algorithms,[26,27] our statement is that current modeling evolution towards 'adaptable objects' through flexibility does not fully satisfy the 'induced-fit' concept, which is essential to understand recognition and interaction processes.[28] Attempts to introduce flexibility in modeling strategies are limited according to the protocol or the

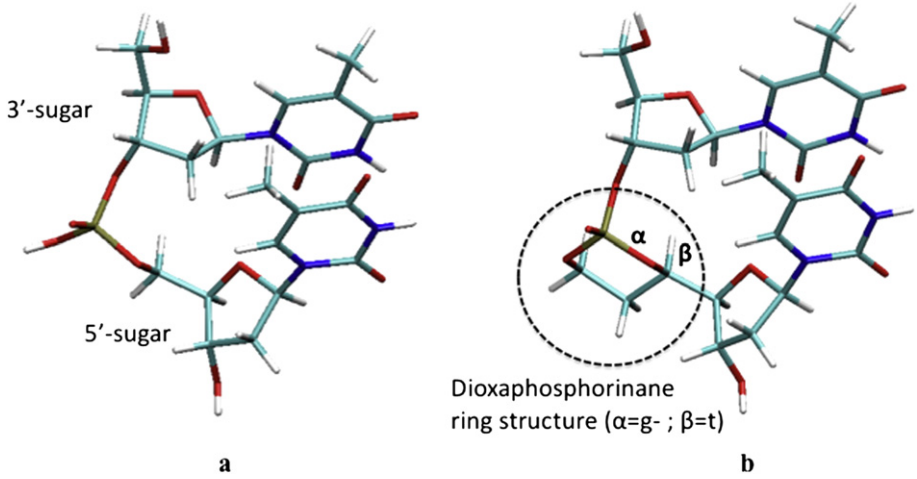

Fig. 1. a) On the left: a 'natural' dinucleotide structure. (b) On the right: its constrained analogue in which α and β torsion angles are restricted by a dioxaphosphorinane ring structure at the canonical conformation (α=*g*−; β=*t*). The dioxaphosphorinane ring consists in a $(CH_2)_2$ shortcut between C5′ and O1 atoms of DNA backbone. These structures are used in this study, both inserted in duplexes (see Section 2.2) and as single strands (see Section 2.3).

In order to test this hypothesis, we follow the experimental example proposed by Dupouy et al.:[24] a thymine−thymine monophosphate dinucleotide. Our goal is to analyze the sugar flexibility and its relation with the backbone modification. The modified form that we consider in this article is a canonical form (α=*g*−=−60±30°; β=*t*=180±30°), mostly found in classical B and A-forms. To study duplex stability and sugar conformational changes, we used the static mode method.[19] The overall goal of static modes is to provide a framework where full molecular flexibility can be obtained in a reasonable computer time. In this view, the static mode approach is an alternative to existing Molecular Dynamics techniques and Normal Mode Analysis based methods. Its main characteristic is to provide a well-defined screening of potential external excitations applied on the investigated molecular object.

In the following section, we briefly introduce the concept of static modes. Subsequently, we discuss the first application of the static mode method dedicated to DNA. Two main aspects are investigated. We first concentrate on the impact of the DNA backbone modification on thermal stability of duplexes; this leads us to a formal and factual validation of experimental results. The role of the sugar rigidity is discussed in the light of these results; we show

operator. By contrast, our method takes into account the full and intrinsic flexibility at the atomic level, and provides deformations guided by local forces. Following the existing computational approaches (e.g., Molecular Dynamics (MD), Normal Mode Analysis (NMA) etc.) dedicated to study the flexible and rigid motifs in biomolecules, we have developed a new computing method: the static mode method (SM) (see Ref. 19 for more technical details).

This method results in the mapping of all possible deformations of a molecule subject to various external excitations. A given mode is related to an excitation on a specific atom in a specific direction, each single mode then corresponds to the collective response to a single excitation. Practically, the calculation is based on the manipulation of force constants that are derived from a given energy model (the method can be used whatever the energy model). Each mode is then stored to be further used and coupled with other modes depending on the type of excitation one operator wishes to investigate. This pre-calculated information (static modes), stored in a data bank, can be used to efficiently anticipate conformational changes arising from external stimuli (pinching, shearing, etc.): to mimic single to multi atomic contacts, mono to multi molecular domain contacts.

In this scheme, the concept of normal modes,[29] which are natural vibrations of a molecule, is abandoned in favor of the permanent deformations caused by interactions with other molecules. Rigorously, MD is suitable to address full flexibility in relation with complex molecular environment (docking, solvent…). However, its limitation comes from the attainable experimental duration that cannot exceed a few nanoseconds when sticking to appropriate energy models. Therefore, only partial flexibility information can be derived from MD simulations as reaction time of biological processes can be in the order of microseconds or higher.[30] The essence of the SM method is to overcome this problem: the idea is to shortcut the determination of the transient vibration and to calculate directly the steady state deformation. In this work, we demonstrate that the static mode method can be employed to precisely understand and quantify the role of DNA modification (D-CNAs type) on global DNA flexible response.

2.2. Duplex stability

The aim of CNAs synthesis is to obtain more stable duplexes. C. Dupouy et al. have evaluated the thermal stability of various duplexes by UV melting-curve analysis. They found that the stability of DNA homoduplexes and DNA/RNA heteroduplexes containing (α=*g*−; β=*t*) restricted nucleotides is improved, and significantly more in the first case, compared to unmodified duplexes.

We consider four duplexes containing a desoxy-thymine dimer d(TpT) and its complementary strand: a DNA homoduplex, a DNA/RNA heteroduplex, and both analogues containing a (α=*g*−; β=*t*) modification inserted in the d(TpT) strand. Each structure results from a classical minimization made with AMBER 8[31] suite of programs in implicit solvent using the ff94 force field. Previous studies have actually proved its ability to describe base stacking and pairing consistently.[32] From these structures, the static modes that are elementary deformations, are calculated and combined to create a specific excitation. Here, our criterion to evaluate duplex stability through static modes is the stretching of the hydrogen bonds between base pairs. Each couple of atoms is pinched to get the resulting hydrogen bond opening between the base pairs. This resulting local deformation in response to pinching excitation is our criterion to evaluate duplex stability. This type of pinching, i.e., the application of a null torque on each couple of atoms, is the most direct and systematic way to simulate a multisite excitation. Besides, in order to get comparable values, all the forces are normalized. For each duplex, we treat four hydrogen bonds, two per base pair: between O4 and H6, and H3 and N1 of thymine and adenine, respectively (according to the IUPAC-IUB recommendations[33]). Bonds numbering is presented on Fig. 2. We get a deformation of the duplex for each pinch applied. For each new structure and for each bond, we calculate the average, over all possible pinches, of the hydrogen bond opening. l_H values presented in Tables 1 and 2 correspond to the opening percentage of each bond, in relation to the equilibrium values, i.e., the starting values.

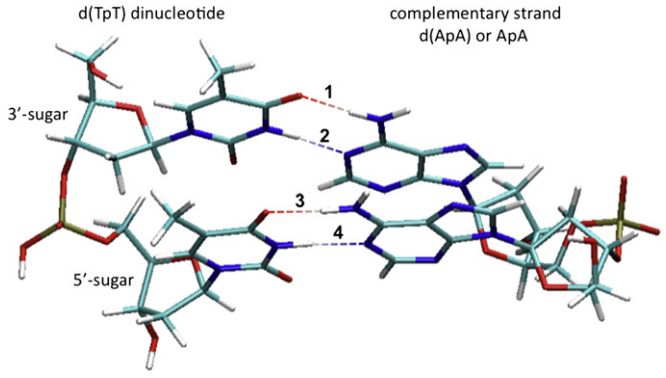

Fig. 2. Numbering of the four considered bonds between the base pairs of nucleic acids duplexes.

Table 1
Hydrogen bonds opening for the four considered bonds between the base pairs of the DNA homoduplex and of the duplex analogue containing a *g*− constraint

	l_H (%) DNA/DNA	l_H (%) DNA/DNA (*g*−)
Bond n°1	2.81	2.57
Bond n°2	5.97	5.73
Bond n°3	2.68	2.62
Bond n°4	5.19	5.27

Table 2
Hydrogen bonds opening for the four considered bonds between the base pairs of the RNA/DNA heteroduplex and of the duplex analogue containing a *g*− constraint in the DNA stand

	l_H (%) RNA/DNA	l_H (%) RNA/DNA (*g*−)
Bond n°1	2.80	2.69
Bond n°2	6.04	5.57
Bond n°3	1.62	1.69
Bond n°4	3.78	3.46

2.3. Sugar flexibility

Furanose ring is highly flexible[34] and known to play a pivotal role between the rigid bases and the flexible backbone of nucleic acids. It exhibits multiple conformations, none of them being planar. These conformations, called puckering modes, can be described by the pseudorotation concept, introduced by Sundaralingam et al.,[35,36] who established relationships between the five endocyclic torsion angles ν_0–ν_4: ν_0: C4′–O4′–C1′–C2′; ν_1: O4′–C1′–C2′–C3′; ν_2: C1′–C2′–C3′–C4′; ν_3: C2′–C3′–C4′–O4′; ν_4: C3′–C4′–O4′–C1′ (see Fig. 3).

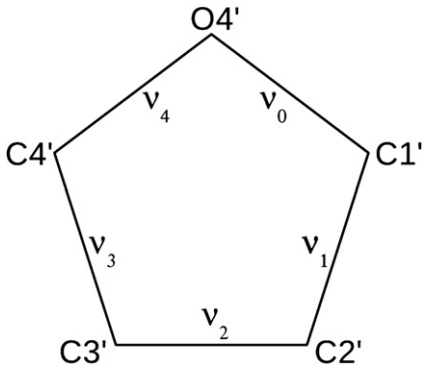

Fig. 3. Furanose ring: scheme of atomic numbers and endocyclic torsion angles.

Puckering modes are thus uniquely defined by two angles: the phase angle of pseudorotation *P* and the maximum out-of-plane pucker ν_{max}, described by Eqs. 1 and 2:

$$\tan P = \frac{(\nu_4+\nu_1)-(\nu_3+\nu_0)}{2\cdot\nu_2\cdot(\sin 36^\circ+\sin 72^\circ)} \quad (1)$$

$$\nu_{max} = \left(\frac{\nu_2}{\cos P}\right) \quad (2)$$

Plotting *P* and ν_{max} on a polar graph, namely a pseudorotation cycle, can represent overall puckering modes as we will show in the following analysis.

In a single strand, furanose ring can be found in different conformations, but, as shown by experimental structures, the main ones are typically $C_{3'}$-*endo* (called *north* by spectroscopists because P is in the range $-1° \leq P \leq 34°$) and $C_{2'}$-*endo* (called *south*, in the range $144° \leq P \leq 180°$).[6] Interestingly, in a duplex, sugars are mostly found in north conformation in A-form duplexes while being in south conformation in B-form duplexes.[37] As we previously mentioned, RNA duplexes are mostly found in the A-form, whereas DNA can switch from B-form to A-form, for example, in a DNA/RNA heteroduplex.

We consider a d(TpT) dinucleotide and its restricted analogue. These structures are presented on Fig. 1 (1a and b, respectively). The AMBER package was first used in this study but did not allow getting accurate details about sugar puckering (results not shown). In view of this, we chose to use a quantum model. The molecular structures and the associated static mode database presented here result from a first-principles-based energy minimization made with GAUSSIAN 03 simulation package[38] using the B3LYP functional[39] and a 6-31++G** basis set. Following the static mode determination, we optimized, for each atom, the direction of the applied force to maximize the phase changes favoring south to north pathway.

3. Results and discussion

3.1. Duplex stability

In Table 1, we compare hydrogen bond opening in a DNA duplex involving an unmodified dimer (left column) with a modified one (right column). In Table 2, the comparison is made between a RNA/DNA duplex and its analogue containing a constrained dinucleotide. In either case, three out of four openings are smaller in the duplex that contains a CNA than in the unmodified one. In DNA homoduplex, opening gains are 0.24, 0.24, and 0.06% for the bonds n°1, 2, and 3, respectively. In RNA/DNA heteroduplex, opening gains are 0.11, 0.47, and 0.32% for the bonds n°1, 2, and 4, respectively. This means that opening three out of four hydrogen bonds is more difficult when a CNA is inserted in a DNA strand. These values argue in favor of an increase of thermal stability of CNA-based duplexes. In a second time, we take an interest in the most stable hydrogen bond of the duplexes, i.e., the most difficult to open, compared to the three others. It is thus legitimate to think that when this bond breaks, both strands of the duplex are ready for mismatching. In the case of DNA homoduplex, the bond n°3, with only 2.68% opening, is the most difficult to open. In DNA duplex involving a modification, the bond n°3 is even more difficult to open than in the natural DNA duplex (2.62% comparing to 2.68%). In this case, the minimal value, obtained for the bond n°1 (2.57%), is lower than the minimal value calculated for the natural DNA duplex, what reinforces the global stability increase. On the contrary, as shown in Table 2, in RNA/DNA heteroduplexes, the most stable bond is also the n°3, but in this case, it is easier to open it in the duplex containing a CNA than in the natural one (1.69% compared to 1.62%). The differences found here are small but we have to keep in mind that they result from normalized forces. As they are treated in the frame of a linear model, a coefficient higher than 1 can be attributed to these force to get a proportional deformation. Besides, experimental values show stability improvement around a few Celsius degrees (5 and 0.9 °C, respectively, in DNA/DNA and RNA/RNA duplexes[24]).

As observed experimentally, the conclusion is that the global stabilizing effect observed when CNAs are inserted into nucleic acids duplexes is however lower in A-type (DNA/RNA heteroduplex) than in B-type (DNA/DNA homoduplex) duplexes. One accepted hypothesis, if not demonstrated, is to explain this difference with a 5′-sugar rigidification hindering a south/north transition.[24] In the next section, we show how static modes make it possible to quantify the possible phase change of 5′-sugar in both unmodified and modified dinucleotides.

3.2. Sugar flexibility

Figs. 4 and 5 show the conformational changes of 5′-sugar in a non-modified and modified d(TpT), respectively. In the equilibrium state (red points), both sugars are in south conformation: P=169.01° and ν_{max}=30.91° for the non-modified dinucleotide, P=167.38° and ν_{max}=30.45° for the constrained dinucleotide. These values are in the range of typical experimental observed values.[36,37] Each black cross on the graph represents a possible change of 5′-sugar conformation after application, on a given atom, of a normalized force with an optimized direction.

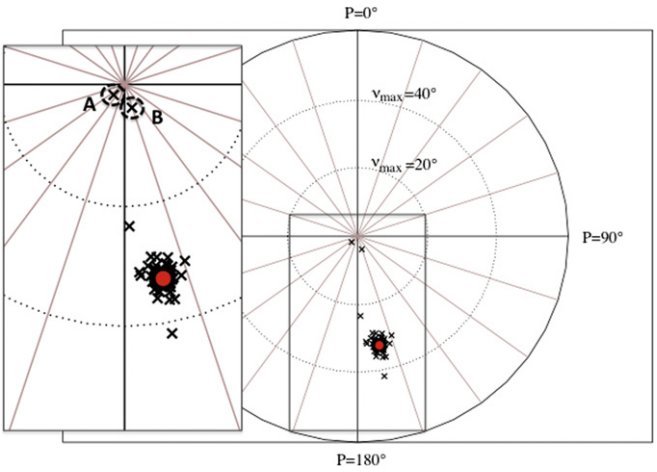

Fig. 4. Pseudorotation cycle of the 5′ furanose ring of a non-modified d(TpT). Red point represents the equilibrium state, black points are the possible conformational changes predicted by the static modes. A zoom is shown on the left.

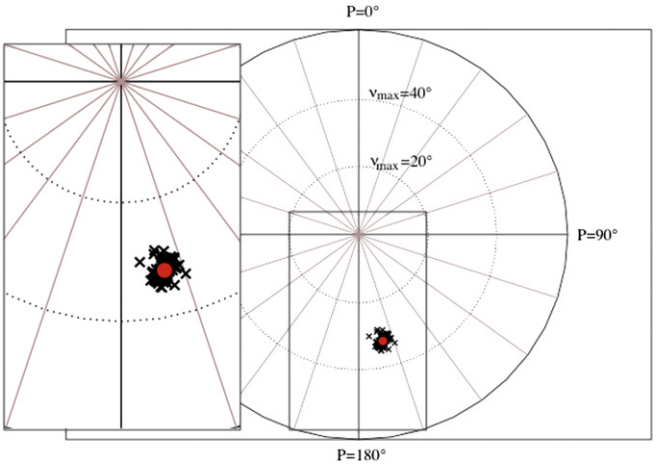

Fig. 5. Pseudorotation cycle of the 5′ furanose ring of a constrained d(TpT). Red point represents the equilibrium state, black points are the possible conformational changes predicted by the static modes. Furanose ring seems to be more rigid in the constrained dinucleotide than in the natural one.

From Figs. 4 and 5, we observe a difference in the distribution of conformations around the equilibrium indicating that the overall conformational response to elementary excitations (i.e., flexibility response to a single excitation) varies drastically upon chemical modification of the backbone. The cloud in the non-modified dinucleotide shows an axial spreading behavior while the

constrained dinucleotide exhibits a very compact distribution around the non-excited dinucleotide. Therefore, it can be concluded that the sugar of the natural dinucleotide is able to change its conformation more easily, at least along a specific axis. On the contrary, the sugar of the constrained dinucleotide is much more rigid and do not exhibit a specific direction to change its conformation, at least through single excitations (i.e., through forces applied on a single atom of the dinucleotide). The existence of such specific directions designed by one or an ensemble of points suggests a natural propensity of the molecule to undergo specific conformational changes and in particular here, a transition from south to north conformation.

3.3. Atomistic mechanisms of the south/north transition

In addition to these global preliminary conclusions, a deeper study of the graphs allows investigating additional details on the propensity of the sugar to undergo phase changes. Each point corresponding to a specific excitation on a specific atom, it becomes possible to map with an atomic precision the local origin of a more global conformational behavior. Notably, focusing on Fig. 4, we can distinguish particular points authorizing a possible transition from south to north conformations (points A and B, Fig. 4). This means that, for a given transition, north/south in this case, it is possible to determine what constraints should be applied so as to obtain the desired transition. Moreover, beyond the elementary excitations envisaged in the present study, it is also possible to draw step-by-step more complex constraints in a manner to optimize further on the desired conformational response. In the present case, one can identify particular points in the graph, i.e., particular puckering modes, and assign to each of them, a specific atom or a population of atoms (through multiple excitation mode) of the molecule as being the source of this deformation.

It is worth noticing here that the points represent permanent deformations due to normalized forces. Phase variations are small since we use the harmonic approximation and stay in local minima. The main focus here is to indicate that a natural south to north conformational 'breathing' does exist under a specific and localized external excitation. In this view, a unique relation between an interaction with the medium and conformational changes can be operated. Therefore, we do not address here the identification of new stable conformations neither reaction pathways. Indeed, as previously said, the static mode method provides a permanent deformation induced by a local excitation. A real pathway could be built by a succession of deformation/minimization steps, which is not the ambition of the present paper.

As a practical example, focusing now on the two points representing the largest conformational changes on Fig. 4 (points A and B), we find that these points correspond to constraints imposed on C5′ and O5′ atoms. The optimized two forces applied to get the variation of pucker associated to these points are shown on Fig. 6. It is noteworthy that the optimum excitations implying the transition are not applied on the sugar ring itself, but are localized on backbone atoms. This result underlines the strong relationship between backbone rearrangement and sugar flexibility, and offers new perspectives in molecular design.

This result is significant, as both atoms C5′ and O5′ are directly involved in the dioxaphosphorinane ring created to rigidify the backbone. It turns out here that atoms whose displacements are forbidden in CNAs enable furanose adaptability. Therefore, static modes indicate that furanose rigidification freezes the modified dinucleotide in the south conformation which agrees well with the experimental observation that thermal stability is improved on homoduplexes while heteroduplexes are moderately affected due to the required south to north transition.

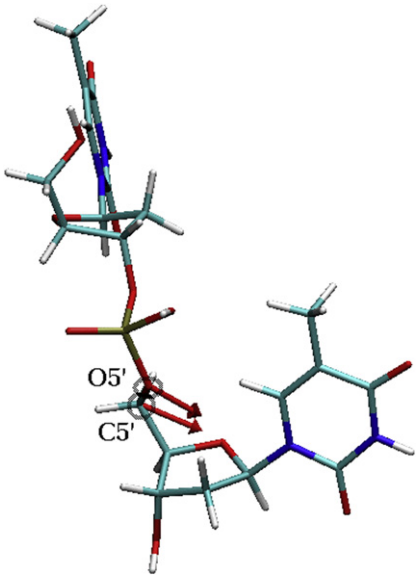

Fig. 6. Representation of the optimized forces applied on C5′ and O5′ atoms of d(TpT) dinucleotide to obtain the maximum phase change of 5′-sugar. These variations correspond to A and B points on Fig. 4.

4. Conclusion

In conclusion, a recently proposed modeling methodology, namely the static mode method is employed to describe DNA flexible response to external excitations. Following recent experiments on modified nucleotides as well as more theoretical considerations on the potential role of nucleosides on overall DNA conformations, we use the static mode technique to give further insights into the intimate relation between local backbone excitations and global DNA behavior. We analyze the effects of the insertion of modified nucleotides (specifically α,β-D-DNA) into DNA/DNA and DNA/RNA duplexes.

We show how static modes can be used and manipulated to give access to general molecular behavior, such as DNA thermal stability. As established by recent experimental results, we show that α,β-D-DNA improve duplexes stability, particularly in the case of B-type duplexes. Then, the furanose-induced DNA flexibility and its traditional treatment through the concept of pseudorotation are revisited through static modes: we map the specific furanose deformation fields necessary to induce selected DNA conformational changes. We particularly address the mapping of excitations inducing south to north conformations. This second step allows us to corroborate the 5′-sugar ridigification hypothesis: we show precisely some potential atomistic mechanisms (C5′ and O5′ displacements in given directions) that are pertinent to envisage further sugar phase change. In structural terms, the static mode method allows us establishing a relation between the backbone rearrangement and the furanose flexibility. Surprisingly, the optimal furanose ring deformation is not obtained through its direct excitation but rather on C5′ and O5′ backbone atoms. This can be more generally extended to investigations where local structural modifications have to be correlated to more global conformational response of biomolecules.

The computational efficiency of the overall simulation procedure (compare to more conventional Molecular Dynamics for instance) opens promising alternatives whenever full atomistic and blind prediction of macromolecular flexibility is needed. We believe that these pre-calculated static deformation modes could be used whenever macromolecular flexibility is an issue as in the present study: screening excitations and understanding biomolecular conformational response.

Funding

This work was supported by the French National Agency for Research (ANR-NANOBIOMOD project) and the French Institute for Advanced Living Sciences (ITAV-ALMA project).

Acknowledgements

We thank CALMIP supercomputer center for CPU resources. We wish to thank Alain Vigroux, Nathalie Iché-Tarrat and Jean-Marc Escudier from LSPCMIB-CNRS for helpful discussions.

Supplementary data

Supplementary data associated with this article can be found in the online version at doi:10.1016/j.tet.2010.09.083.

References and notes

1. Sara, A.; Kono, H. *Annu. Rev. Biophys. Biomol. Struct.* **2005**, *34*, 379–398.
2. Luscombe, N. M.; Austin, S. E.; Berman, H. M.; Thornton, J. M. *Genome Biol.* **2000**, *1*, 1–7.
3. Cram, D. J. *Angew. Chem., Int. Ed. Engl.* **1988**, *27*, 1009–1020.
4. Kool, E. T. *Chem. Rev.* **1997**, *97*, 1473–1488.
5. Gabb, A.; Harvey, S. C. J. *Am. Chem. Soc.* **1993**, *115*, 4218–4227.
6. Saenger, W. *Principles of Nucleic Acid Structure*; Springer-Verlag: New York, NY, 1984.
7. Tarkoy, M.; Bolli, M.; Schweizer, B.; Leumann, C. *Helv. Chim. Acta* **1993**, *76*, 481–510.
8. Bolli, M.; Lubini, P.; Leumann, C. *Helv. Chim. Acta* **1995**, *78*, 2077–2096.
9. Wengel, J.; Petersen, M.; Nielsen, K. E.; Jensen, G. A.; Hakansson, A. E.; Kumar, R.; Sorensen, M. D.; Rajwanshi, V. K.; Bryld, T.; Jacobsen, J. P. *Nucleosides, Nucleotides Nucleic Acids* **2001**, *20*, 389–396.
10. Leumann, C. J. *Bioorg. Med. Chem.* **2002**, *10*, 841–854.
11. Singh, S. K.; Koshkin, A. A.; Wengel, J.; Nielsen, P. *Chem. Commun.* **1998**, 455–456.
12. Koshkin, A. A.; Singh, S. K.; Nielsen, P.; Rajwanshi, V. K.; Kumar, R.; Meldgaard, M.; Erik Olsen, C.; Wengel, J. *Tetrahedron* **1998**, *54*, 3607–3630.
13. Osaki, T.; Obika, S.; Harada, Y.; Mitsuoka, Y.; Sugaya, K.; Sekiguchi, M.; Roongjang, S.; Imanishi, T. *Tetrahedron* **2007**, *63*, 8977–8986.
14. van Well, R. M.; Meijer, M. E. A.; Overkleeft, H. S.; van Boom, J. H.; van der Marel, G. A.; Overhand, M. *Tetrahedron* **2003**, *59*, 2423–2434.
15. Freitag, M.; Thomasen, H.; Christensen, N. K.; Petersen, M.; Nielsen, P. *Tetrahedron* **2004**, *60*, 3775–3786.
16. Fressigné, C.; Piettre, S.; Condamine, E.; Altona, C.; Gautier, A. *Tetrahedron* **2005**, *61*, 4769–4777.
17. Ellington, A. D.; Szostak, J. W. *Nature* **1990**, *346*, 818–822.
18. Egholm, M.; Buchardt, O.; Christensen, L.; Behrens, C.; Freier, S. M.; Driver, D. A.; Berg, R. H.; Kim, S. K.; Norden, B.; Nielsen, P. E. *Nature* **1993**, *365*, 566–568.
19. Brut, M.; Estève, A.; Landa, G.; Renvez, G.; Djafari Rouhani, M. *Eur. Phys. J. E.* **2009**, *28*, 17–25.
20. Sùrensen, A. M.; Nielsen, K. E.; Vogg, B.; Jacobsen, J. P.; Nielsen, P. *Tetrahedron* **2001**, *57*, 10191–10201.
21. Le Clézio, I.; Escudier, J.-M.; Vigroux, A. *Org. Lett.* **2003**, *5*, 161–164.
22. Le Clézio, I.; Gornitzka, H.; Escudier, J.-M.; Vigroux, A. *Org. Chem.* **2003**, *70*, 1620–1629.
23. Dupouy, C.; Le Clézio, I.; Lavedan, P.; Gornitzka, H.; Escudier, J.-M.; Vigroux, A. *Eur. J. Org. Chem.* **2006**, *12*, 5515–5525.
24. Dupouy, C.; Iché-Tarrat, N.; Durrieu, M.-P.; Rodriguez, F.; Escudier, J.-M.; Vigroux, A. *Angew. Chem.* **2006**, *118*, 3705–3709.
25. Dupouy, C.; Iché-Tarrat, N.; Durrieu, M.-P.; Vigroux, A.; Escudier, J.-M. *Org. Biomol. Chem.* **2008**, *6*, 2849–2851.
26. Bonvin, A. M. J. J. *Curr. Opin. Struct. Biol.* **2006**, *16*, 194–200.
27. Orozco, M.; Pérez, A.; Noy, A.; Luque, F. J. *Chem. Soc. Rev.* **2003**, *32*, 350–364.
28. Csermely, P.; Palotai, R.; Nussinov, R. *Trends Biochem. Sci.* **2010**, *35*, 539–546.
29. Tama, F.; Sanejouand, Y.-H. *Protein Eng.* **2001**, *14*, 1–6.
30. Karplus, M.; McCammon, J. *Nat. Struct. Biol.* **2002**, *9*, 646–652.
31. Case, D. A.; Darden, T. A.; Cheatham, I. T. E.; Simmerling, C. L.; Wang, J.; Duke, R. E.; Luo, R.; Merz, K. M.; Wang, B.; Pearlman, D. A.; Crowley, M.; Brozell, S.; Tsui, V.; Gohlke, H.; Mongan, J.; Hornak, V.; Cui, G.; Beroza, P.; Schafmeister, C.; Caldwell, J. W.; Ross, W. S.; Kollman, P. A. *AMBER 8*; University of California: San Francis, 2004.
32. Sponer, J.; Jurecka, P.; Hobza, P. *J. Am. Chem. Soc.* **2004**, *126*, 10142–10151.
33. IUPAC-IUB Commission on Biochemical Nomenclature (CBN) Abbreviations and symbols for description of conformation of polypeptide chains *Pure Appl. Chem.* **1974**, *40*, 291–308.
34. Levitt, M.; Warshel, A. *J. Am. Chem. Soc.* **1978**, *100*, 2607–2613.
35. Altona, C.; Sundaralingam, M. *J. Am. Chem. Soc.* **1972**, *94*, 8205–8212.
36. Rao, S.; Westhof, E.; Sundaralingam, M. *Acta Crystallogr.* **1981**, *A37*, 421–425.
37. Arora, K.; Schlick, T. *Chem. Phys. Lett.* **2003**, *378*, 1–8.
38. Frisch, M. J.; Trucks, G. W.; Schlegel, H. B.; Scuseria, G. E.; Robb, M. A.; Cheeseman, J. R.; Montgomery, J. A.; Vreven, T.; Kudin, K. N.; Burant, J. C.; Millam, J. M.; Iyengar, S. S.; Tomasi, J.; Barone, V.; Mennucci, B.; Cossi, M.; Scalmani, G.; Rega, N.; Petersson, G. A.; Nakatsuji, H.; Hada, M.; Ehara, M.; Toyota, K.; Fukuda, R.; Hasegawa, J.; Ishida, M.; Nakajima, T.; Honda, Y.; Kitao, O.; Nakai, H.; Klene, M.; Li, X.; Knox, J. E.; Hratchian, H. P.; Cross, J. B.; Bakken, V.; Adamo, C.; Jaramillo, J.; Gomperts, R.; Stratmann, R. E.; Yazyev, O.; Austin, A. J.; Cammi, R.; Pomelli, C.; Ochterski, J. W.; Ayala, P. Y.; Morokuma, K.; Voth, G. A.; Salvador, P.; Dannenberg, J. J.; Zakrzewski, V. G.; Dapprich, S.; Daniels, A. D.; Strain, M. C.; Farkas, O.; Malick, D. K.; Rabuck, A. D.; Raghavachari, K.; Foresman, J. B.; Ortiz, J. V.; Cui, Q.; Baboul, A. G.; Clifford, S.; Cioslowski, J.; Stefanov, B. B.; Liu, G.; Liashenko, A.; Piskorz, P.; Komaromi, I.; Martin, R. L.; Fox, D. J.; Keith, T.; Al-Laham, M. A.; Peng, C. Y.; Nanayakkara, A.; Challacombe, M.; Gill, P. M. W.; Johnson, B.; Chen, W.; Wong, M. W.; Gonzalez, C.; Pople, J. A. *Gaussian03 Rev C.01*; Gaussian: Pittsburgh, 2003.
39. Becke, A. D. *J. Chem. Phys.* **1993**, *98*, 1372–1377.